AD_____

Award Number: DAMD17-03-1-0297

TITLE: Genomic and Expression Profiling of Benign and Malignant Nerve Sheath Tumors in Neurofibromatosis Patients

PRINCIPAL INVESTIGATOR: Matt J. Van De Rijn, M.D., Ph.D.
Torsten Neilsen, M.D., Ph.D.
Brian Rubin, M.D., Ph.D.

CONTRACTING ORGANIZATION: Stanford University School of Medicine
Stanford, CA 94304-5401

REPORT DATE: May 2005

TYPE OF REPORT: Annual

PREPARED FOR: U.S. Army Medical Research and Materiel Command
Fort Detrick, Maryland 21702-5012

REPORT DOCUMENTATION PAGE

Form Approved
OMB No. 074-0188

1. AGENCY USE ONLY (Leave blank)	2. REPORT DATE	3. REPORT TYPE AND DATES COVERED
	May 2005	Annual (1 May 2004 - 30 Apr 2005)

4. TITLE AND SUBTITLE
Genomic and Expression Profiling of Benign and Malignant Nerve Sheath Tumors in Neurofibromatosis Patients

5. FUNDING NUMBERS
DAMD17-03-1-0297

6. AUTHOR(S)
Matt J. Van De Rijn, M.D., Ph.D.
Torsten Neilsen, M.D., Ph.D.
Brian Rubin, M.D., Ph.D.

7. PERFORMING ORGANIZATION NAME(S) AND ADDRESS(ES)
Stanford University School of Medicine
Stanford, CA 94304-5401

E-Mail: mrijn@stanford.edu

8. PERFORMING ORGANIZATION REPORT NUMBER

9. SPONSORING / MONITORING AGENCY NAME(S) AND ADDRESS(ES)
U.S. Army Medical Research and Materiel Command
Fort Detrick, Maryland 21702-5012

10. SPONSORING / MONITORING AGENCY REPORT NUMBER

11. SUPPLEMENTARY NOTES
Original contains color plates: All DTIC reproductions will be in black and white.

12a. DISTRIBUTION / AVAILABILITY STATEMENT
Approved for Public Release; Distribution Unlimited

12b. DISTRIBUTION CODE

13. ABSTRACT (Maximum 200 Words)

The goal of the study is to identify genes that will serve as molecular markers for progression of neurofibroma to MPNST, and to identify potential therapeutic targets. Gene expression profiling was performed on 26 cases of MPNSTs, 23 schwannomas, 20 neurofibromas and 11 synovial sarcomas. By using unsupervised hierarchical clustering most tumors were grouped together according to tumor type. Further analysis suggested that a major trend in transformation from neurofibroma towards MPNST is accompanied by the loss of gene expression in a large number of genes, rather than widespread de novo expression of genes upon transformation. Subsequent analyses using Significance Analysis of Microarrays (SAM) identified genes that differentiate various nerve sheath tumors. The analysis also indicated new subtypes of MPNSTs. Expression of genes associated with TFGB signaling in majority of neurofibromas but not in MPNST suggest that TGFB signaling is one of the key regulatory pathways in neurofibromas. A large tissue microarray (TMA) was made containing 200 nerve sheath tumors and is being tested by IHC and ISH markers.

14. SUBJECT TERMS
Gene microarrays, expression profiling, tissue microarrays, in situ hybridization immunochemistry, arrayCGH

15. NUMBER OF PAGES
32

16. PRICE CODE

17. SECURITY CLASSIFICATION OF REPORT	18. SECURITY CLASSIFICATION OF THIS PAGE	19. SECURITY CLASSIFICATION OF ABSTRACT	20. LIMITATION OF ABSTRACT
Unclassified	Unclassified	Unclassified	Unlimited

Table of Contents

Award Number: DAMD17-03-1-0297

Title: Genomic and Expression Profiling of Benign and Malignant Nerve Sheath Tumors in Neurofibromatosis Patients.

INTRODUCTION

Malignant peripheral nerve sheath tumors (MPNSTs) are aggressive soft tissue tumors (STT) that arise from neurofibromas in patients with neurofibromatosis (Riccardi 1981; Cichowski and Jacks 2001). Malignant transformation is a life threatening complication in patients with neurofibromatosis. The transformation of neurofibromas into MPNSTs is not understood on a molecular level. Studies in human and mouse models have revealed that schwann cells are the primary neoplastic cell type in neurofibromas and MPNSTs. The development of MPNST involves mutations of multiple tumor suppressor genes such as NF1. However, it is widely believed that mutations in tumor suppressors alone are not enough to induce peripheral nerve sheath tumor formation. The objective of the study is to identify gene(s) that will serve as a molecular marker for patients in which the benign neurofibroma is progressing towards MPNST. In addition we expect to identify potential therapeutic targets. The techniques used consist of expression profiling on 42000 spot cDNA gene arrays and comparative genome hybridization using the same arrays. These two techniques are used to identify genes of interest. The significance of these genes will then be validated on tissue microarrays (TMAs) using immunohistochemistry and in situ hybridization. Towards this goal, we have in the past year collected frozen tissue samples from patients with MPNST, neurofibroma, schwannoma and synovial sarcoma. As a result we have in the past year significantly increased the number of specimens analyzed on gene arrays for expression profiling. For example, in our first "Annual Report" (which actually described the work in one month due to delays in IRB approval), we reported gene array data for 6 MPNSTs. In the past year we have been able to analyze an additional 20 cases. We have made significant increases in the number of other tumors studied as well. For the construction of nerve sheath tumor TMA, we have also collected large number of paraffin embedded tissue from over 200 patients with nerve sheath tumors.

BODY

Specific aim 1: Genome wide search for genes in nerve sheath tumor

Gene expression profiling of nerve sheath tumors

Gene expression profiling using 42000 spot cDNA microarrays was performed on 26 MPNSTs, 23 schwannomas, 20 neurofibromas and 11 synovial sarcomas (Figure 1, 2). The data from all 80 gene arrays that were generated for this project are stored in the Stanford microarray database facility (http://genome-www5.stanford.edu). The gene expression data was passed through a series of

filters that remove the genes that are poorly measured and remove the genes that show no significant variation across the samples. Control and empty spots on the arrays were not included for the analysis, as well as those spots manually flagged as 'not measurable.' Only cDNA spots with a ratio of signal over background of at least 2.0 in either the Cy3 or Cy5 channel were included. Genes with less than 80% well measured data were not selected. A final filtering criterion was for genes whose expression level differed by at least five fold in at least 3 arrays. Unsupervised hierarchical clustering analysis (Eisen et al 1998) and Significance Analysis of Microarrays (SAM) (Tusher et al 2001) were then performed as described previously (West et al 2005).

Gene array analysis

After passing the predetermined filtering criteria of: 1) ratio of 2.0 mean fluorescence intensity vs. background intensity for each spot in either Cy3 or Cy5 channels and 2) an absolute value of greater than five-fold expression, relative to the mean expression across all 80 cases; in at least 3 samples, 6376 spots remained from the initial dataset. A further selection for genes that had at least 80% measurable data left 4137 genes that passed all the filtering criteria. It should be noted that these are rather stringent selection criteria and that despite this high stringency a large number of genes passed the filtering. This indicates that there are significant number of genes that vary between the different tumors. The 4137 genes and 80 tumor samples were grouped using unsupervised hierarchical clustering, an analysis that clusters the genes into groups with similar expression patterns across the tumors tested and clusters the tumor specimens based on their gene expression profile. The resulting heat map with dendrogram of all 4137 genes and 80 tumors is shown in Figure 2.

By using unsupervised hierarchical clustering most tumors were grouped together according to tumor type (Figure 1 and 2). Two main branches were seen in the cluster. The majority of neurofibromas clustered in one branch. In the second branch, MPNSTs clustered closely with synovial sarcomas leaving the schwannomas to form a distinct group of tumors (Figure 2). The differential expression pattern of the 4137 genes shown in figure 2 indicates that a majority of genes are highly expressed in neurofibromas. MPNSTs and synovial sarcoma (SS) showed relatively a fewer number of genes that highly expressed in these tumors. These findings suggest that the major trend in transformation from neurofibroma towards MPNST is accompanied by loss of gene expression, rather than the expression of previously identified genes. We have encountered this phenomenon in other tumor systems such as the ovary (Gilks et al 2005) and this will obviously complicate the search for MPNST specific markers. Moreover a detailed search for such genes is still ongoing.

Significance Analysis of Microarrays

We subsequently analyzed the expression data by Significance Analysis of Microarrays [SAM] (Tusher et al., 2001), to identify and rank order the genes that differentiate nvarious nerve sheath tumors based on their gene expression

profiles. Using data from all 80 arrays, four SAM analyses were performed. First, we considered all the MPNSTs as a group distinct from the other tumors. Second, we analyzed genes that separated neurofibromas from the other cases. Third, we investigated the genes specifically expressed in schwannomas. Finally, the genes that distinguished SS from the others were identified. The partial lists of highest ranking genes identified in these four separate SAM analyses are shown in Tables 1a, 1b, 1c and 1d respectively. These analyses should be seen as quite preliminary and many more will be performed in the years to come. Nevertheless, these analyses allowed us to make the following 3 observations.

1. Gene expression modules of MPNST vs. neurofibroma

In order to identify the set of genes that are involved in malignant transformation of neurofibromas, we carried out separate clustering of 26 MPNSTs together with 20 neurofibromas (Figure 3). The majority of the MPNSTs, consisting of 17 cases (branch A, Figure 3) clustered as a distinct entity compared with neurofibromas (branch B, Figure 3). However, a subset of 9 cases of MPNSTs clustered along with neurofibromas in branch B. These findings suggests that the MPNSTs in branch B are in the process of malignant transformation. To identify the set of genes that are possibly involved in malignant transformation, we did three separate groups of SAM on these 46 arrays. First, all the MPNSTs in the cluster were considered as a single group of tumors, i.e. MPNSTs were considered as one class and were compared with the neurofibromas (Table 2a). Second, the MPNSTs on each branch A and B were considered as separate entities. SAM was carried on the 17 MPNSTs that clustered in branch A of Figure 3 was compared with the rest of neurofibromas in branch A of the cluster (Table 2b). Finally, SAM was carried on the 9 MPNSTs in branch B with the neurofibromas in branch B (Table 2c). The genes identified through these SAM analyses will be further evaluated with the use of immunohistochemistry and in situ hybridization on our TMA.

2. Possible subtypes in MPNSTs

The findings shown in Figure 3, could also be interpreted as indicative of the existence of different subtypes of MPNST. In order to further examine the possibility of molecular subtypes of MPNSTs we clustered all 26 MPNSTs and found at least two subtypes of MPNSTs. (Figure 4). The distinction between the subtypes was defined by the expression of 906 genes using the same filtering criteria defined above. Only a subset of these 906 genes is shown in Figure 4. We have yet to determine the NF1 status of all the MPNSTs, to determine whether the clustering of MPNST is based on the NF1 status. However, preliminary data with the scanned NF1 status information currently available suggests there is no clustering based on NF1 or sporadic cases. The same MPNSTs that clustered along with neurofibromas in Figure 3 were also clustering separately (in branch B) Figure 4.

3. TFGB signaling pathway in neurofibromas

In our gene expression analysis we noticed the high levels of expression of TGFBR1 and TGFBR2 genes. We further evaluated the expression of genes that are associated with TFGB signaling pathways (Figure 5) in our nerve sheath tumors. The analysis revealed that the majority of neurofibromas expressed genes associated with TFGB signaling suggesting the TGFB signaling is one of the key pathways in neurofibromas. The expression profiles of the TFGB signaling genes are shown in Figure 6. Transforming growth factor-beta (TGF-beta) superfamily signaling plays a critical role in the regulation cell growth, differentiation, and development in a wide range of biological systems. TGF-beta regulates growth and proliferation of cells blocking growth of many cell types. The TGF-beta receptor includes type 1 and type 2 subunits that are serine-threonine kinases and that signal through the SMAD family of transcriptional regulators. Defects in TGF-beta signaling, includes mutation in SMADs, have been associated with cancer in humans (Massague 2000). We will further evaluate the involvement of this pathway using ISH and IHC on our TMA.

Expression of kinase genes in nerve sheath tumors

The human kinome consists of about 514 kinase genes represented as various gene families. Several sarcomas exist in which tyrosine kinase genes are mutated, for example, KIT and PDFGRA in gastrointestinal stromal tumors. Based on an extensive literature search we generated a list of 514 kinase genes. Of the 514 genes 409 are represented on the gene array that we use in our analysis. By using unsupervised hierarchical clustering most tumors were grouped together according to tumor type based on the expression patterns on 409 kinase genes (Figure 7). Further studies are necessary to show any association of kinase expression in various nerve sheath tumors. The clinical relevance of this approach lies in the fact that several soft tissue tumors respond to drugs that target tyrosine kinase receptors.

Development of concept grant proposal

During these studies we compared the gene lists identified on nerve sheath tumor to those derived from a parallel project on smooth muscle tumors performed in the van de Rijn laboratory, and noticed a remarkable overlap. This finding suggested the possibility that similar genes are involved in the transformation in these two different tumor systems. The funding for the annual grant does not support the labor intensive analyses that are needed to validate this hypothesis. As a result we recently submitted a concept grant proposal to support salary for one postdoctoral fellow to intensively study the overlaps, on a gene–by–gene basis using a variety of bioinformatical tools and TMA analyses.

Specific Aim 2: Validation of candidate genes on large numbers of cases using immunohistochemistry and *in situ* hybridization on TMA.

Construction of nerve sheath tumor tissue array

TMAs form excellent tools to validate and extend findings from gene array studies because of paraffin embedded archival material is easier to collect than fresh frozen material used. In previous studies we have developed extensive experience with this approach (West et al 2004; West et al 2005; Subramanian et al 2004; Subramanian et al 2005; Nielsen et al 2004; van de Rijn et al 2002). We decided to construct a tissue microarray (TA-138) consisting of nerve sheath tumors. The TMA was constructed as part of a close collaboration between the Stanford group and the funded collaborators at University of Washington (Brian Rubin) and University of British Columbia (Torsten Nielsen). As a result we now have access to what to our knowledge is the largest TMA of nerve sheath tumors. TA-138 contains 68 MPNSTs, 42 neurofibromas, 22 schwannomas and 15 synovial sarcomas. All the cases were represented in duplicate cores of 0.6mm diameter.

ISH probes for MPNST, schwannoma and synovial sarcomas

In situ hybridization technique is a way in which we can examine and validate the expression of new genes identified through gene microarrays. We recently have been able to design a highly successful in situ hybridization protocol that can be performed on paraffin embedded tissue (West et al 2004; Subramanian et al 2004; Subramanian et al 2005). In selecting the best candidates for in situ hybridization we choose genes that score highly by SAM analysis for their differential expression among different tumor groups. In addition we then select genes that have a high level of expression as measured by a high level of fluorescence in the Cy5 channel on the original gene array data. Using this approach an success rate for generating probes that show reactivity in ISH is about 80%.

From the gene array data we have identified genes (EGFR, CTHRC1, ZIC1, IGF2 and DLK1) that are highly expressed in at least a subset of MPNSTs. We have made an ISH probe against these genes and we have validated them in our tissue array TA-138. Likewise for schwannoma ISH probes were made against genes MAL, SOX10 and CSF1R. For synovial sarcoma we have generated probes for ZIC2, SSX1, TLE1, AUST2, EFNB3 and MSX2. These genes are identified as differentially expressed genes in various nerve sheath tumors. Probes tested on TMA-138 and their respective percent positive staining for each tumor tissue is shown as graph in Figure 8. Further testing of additional probes is necessary to validate the genes as diagnostic markers.

Unique case of MPNST with a novel SSX1 and SYT fusion

From the clusters that were generated from the gene expression data, we notice that a subset of MPNST clusters tightly with synovial sarcomas. In order to exclude the possibility of the missed diagnosis and to confirm the presence of

SSX1 and SYT fusion transcript, we carried out RT-PCR for the diagnostic t(X;18) in synovial sarcoma from the cDNA made from the RNA of frozen tissues used in our gene arrays.

RT-PCR study revealed that except for one SS case (STT108), all the other SS had a SSX1-SYT fusion transcript. The PCR products were sequenced and the fusion was confirmed. For all the synovial sarcoma cases (except STT108), we found the expected size of SSX-SYT fusion transcript of 585 base pairs, using the primer sets SYT: CAACAGCAAGATGCATACCA and SSX consensus primer: CACTTGCTATGCACCTGATG. We noticed a smaller fragment of 297 base pairs fragment in one of our MPNST cases (STT3994) and sequenced the PCR product and found that a novel previously undescribed fusion of SYT exon 8 to SSX1 exon 7 (Figure 9). Further work is needed to show whether the case is indeed an MPNST or whether it represents an intermediate tumor class.

Figure 1

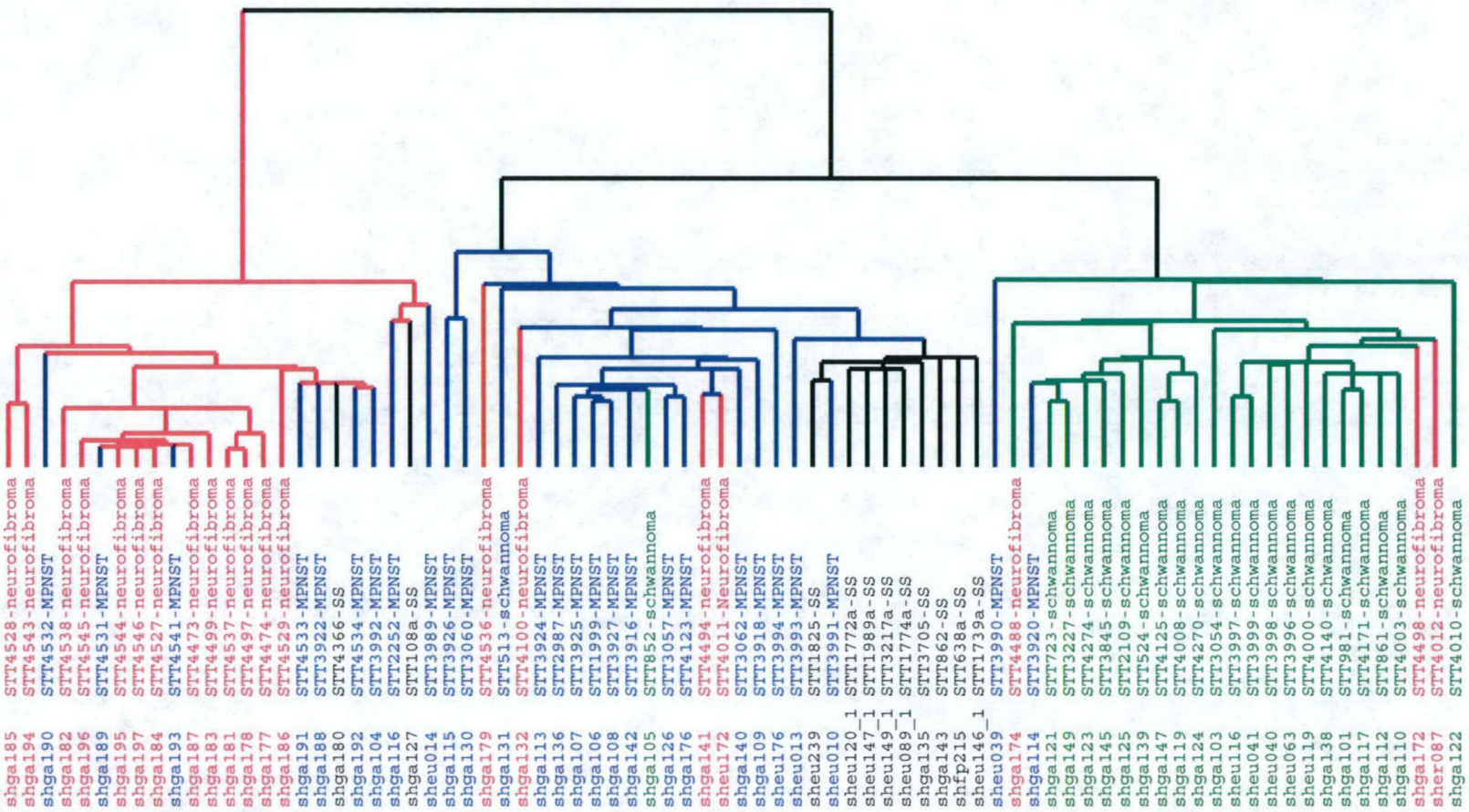
shga185 STT4528-neurofibroma
shga194 STT4543-neurofibroma
shga190 STT4532-MPNST
shga182 STT4538-neurofibroma
shga196 STT4545-neurofibroma
shga189 STT4531-MPNST
shga195 STT4544-neurofibroma
shga197 STT4546-neurofibroma
shga184 STT4527-neurofibroma
shga193 STT4541-MPNST
shga187 STT4473-neurofibroma
shga183 STT4499-neurofibroma
shga181 STT4537-neurofibroma
shga178 STT4497-neurofibroma
shga177 STT4474-neurofibroma
shga186 STT4529-neurofibroma
shga191 STT4533-MPNST
shga188 STT3922-MPNST
shga180 STT4366-SS
shga192 STT4534-MPNST
shga104 STT3992-MPNST
shga116 STT2252-MPNST
shga127 STT108a-SS
sheu014 STT3989-MPNST
shga115 STT3926-MPNST
shga130 STT3060-MPNST
shga179 STT4536-neurofibroma
shga131 STT513-schwannoma
shga132 STT4100-neurofibroma
shga113 STT3924-MPNST
shga136 STT2987-MPNST
shga107 STT3925-MPNST
shga106 STT1999-MPNST
shga108 STT3927-MPNST
shga142 STT3916-MPNST
shga105 STT852-schwannoma
shga126 STT3057-MPNST
shga176 STT4123-MPNST
shga141 STT4494-neurofibroma
sheu172 STT4011-Neurofibroma
shga140 STT3062-MPNST
shga109 STT3918-MPNST
sheu176 STT3994-MPNST
sheu013 STT3993-MPNST
sheu239 STT1825-SS
sheu010 STT3991-MPNST
sheu120_1 STT1772a-SS
sheu147_1 STT1989a-SS
sheu149_1 STT3217a-SS
sheu089_1 STT1774a-SS
shga135 STT3705-SS
shga143 STT862-SS
shfp215 STT638a-SS
sheu146_1 STT1739a-SS
sheu039 STT3990-MPNST
shga174 STT4488-neurofibroma
shga114 STT3920-MPNST
shga121 STT723-schwannoma
shga149 STT3227-schwannoma
shga123 STT4274-schwannoma
shga145 STT3845-schwannoma
shga125 STT2109-schwannoma
shga139 STT524-schwannoma
shga147 STT4125-schwannoma
shga119 STT4008-schwannoma
shga124 STT4270-schwannoma
shga103 STT3054-schwannoma
sheu116 STT3997-schwannoma
sheu041 STT3999-schwannoma
sheu040 STT3998-schwannoma
sheu063 STT3996-schwannoma
sheu119 STT4000-schwannoma
shga138 STT4140-schwannoma
shga101 STT981-schwannoma
shga117 STT4171-schwannoma
shga112 STT861-schwannoma
shga110 STT4003-schwannoma
shga172 STT4498-neurofibroma
sher087 STT4012-neurofibroma
shga122 STT4010-schwannoma

Figure 2

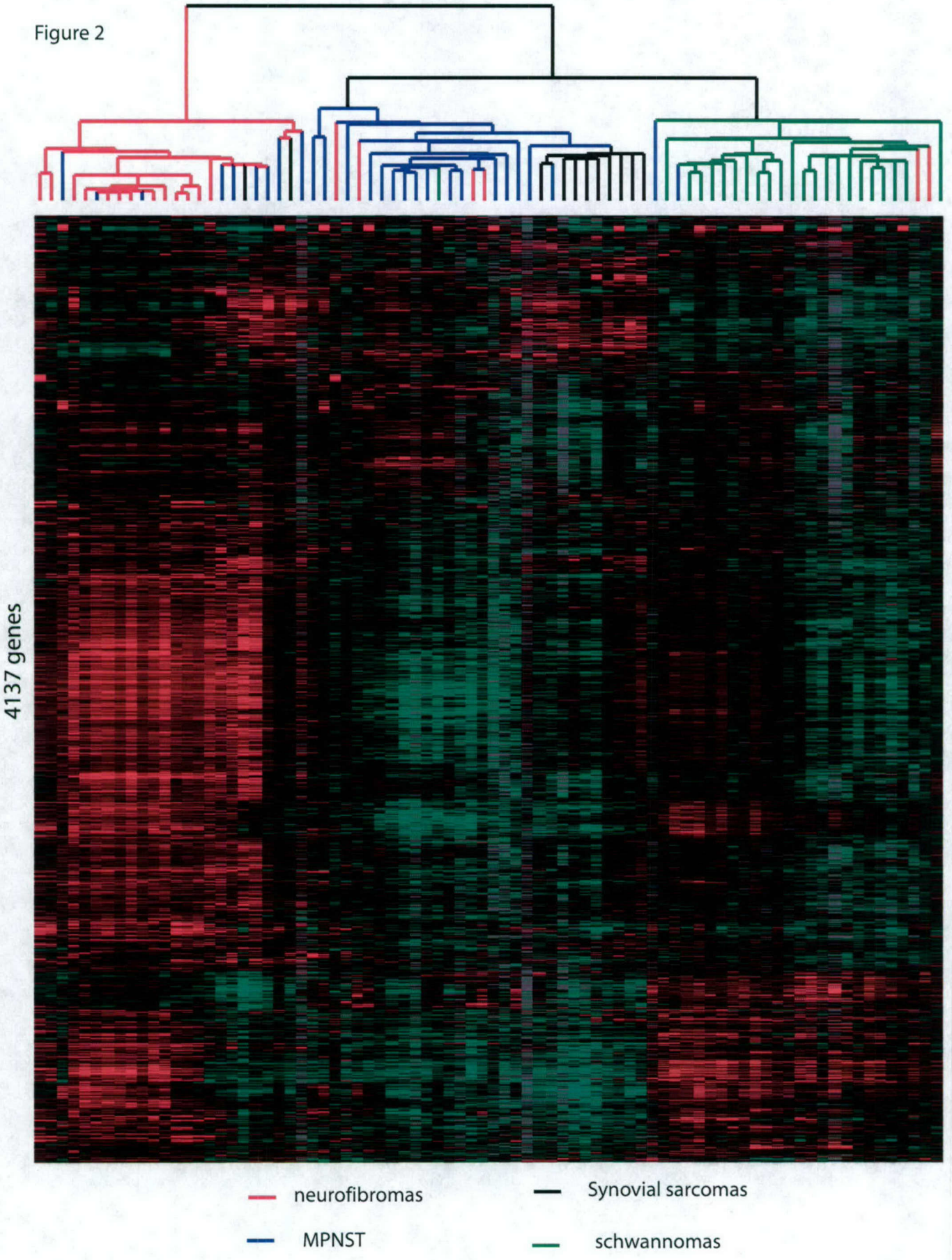
4137 genes
neurofibromas
MPNST
Synovial sarcomas
schwannomas

Figure 3

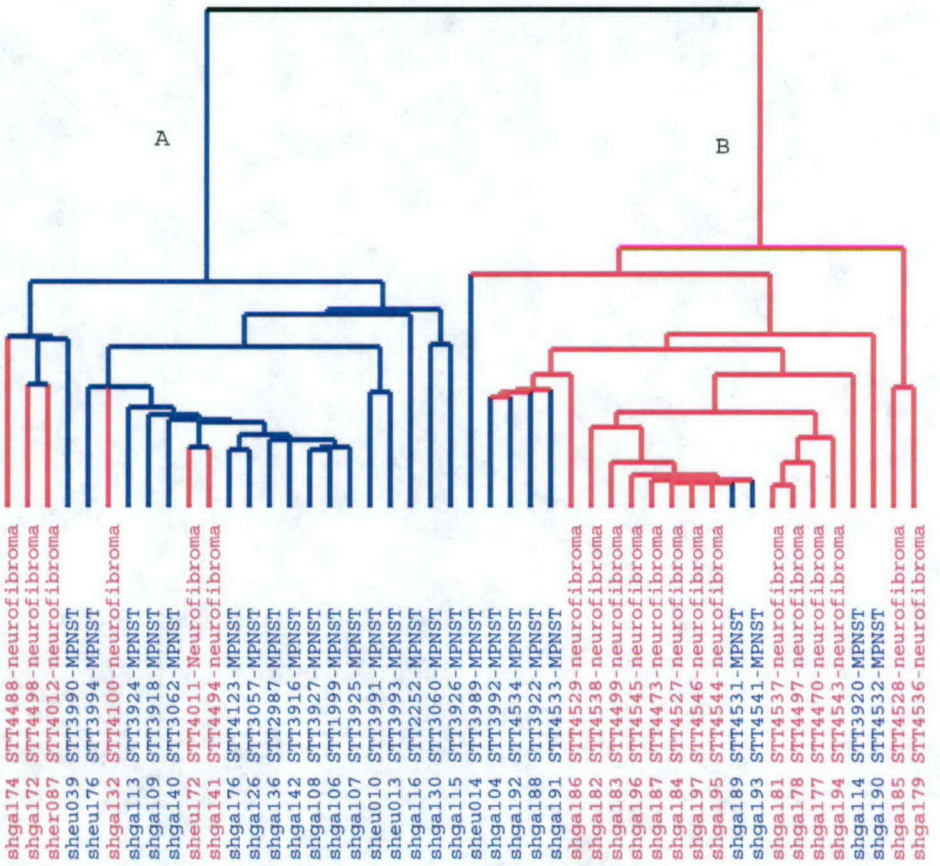
A
B
shga174 STT4488-neurofibroma
shga172 STT4498-neurofibroma
sher087 STT4012-neurofibroma
sheu039 STT3990-MPNST
sheu176 STT3994-MPNST
shga132 STT4100-neurofibroma
shga113 STT3924-MPNST
shga109 STT3918-MPNST
shga140 STT3062-MPNST
sheu172 STT4011-Neurofibroma
shga141 STT4494-neurofibroma
shga176 STT4123-MPNST
shga126 STT3057-MPNST
shga136 STT2987-MPNST
shga142 STT3916-MPNST
shga108 STT3927-MPNST
shga106 STT1999-MPNST
shga107 STT3925-MPNST
sheu010 STT3991-MPNST
sheu013 STT3993-MPNST
shga116 STT2252-MPNST
shga130 STT3060-MPNST
shga115 STT3926-MPNST
sheu014 STT3989-MPNST
shga104 STT3992-MPNST
shga192 STT4534-MPNST
shga188 STT3922-MPNST
shga191 STT4533-MPNST
shga186 STT4529-neurofibroma
shga182 STT4538-neurofibroma
shga183 STT4499-neurofibroma
shga196 STT4545-neurofibroma
shga187 STT4473-neurofibroma
shga184 STT4527-neurofibroma
shga197 STT4546-neurofibroma
shga195 STT4544-neurofibroma
shga189 STT4531-MPNST
shga193 STT4541-MPNST
shga181 STT4537-neurofibroma
shga178 STT4497-neurofibroma
shga177 STT4470-neurofibroma
shga194 STT4543-neurofibroma
shga114 STT3920-MPNST
shga190 STT4532-MPNST
shga185 STT4528-neurofibroma
shga179 STT4536-neurofibroma

Figure 4

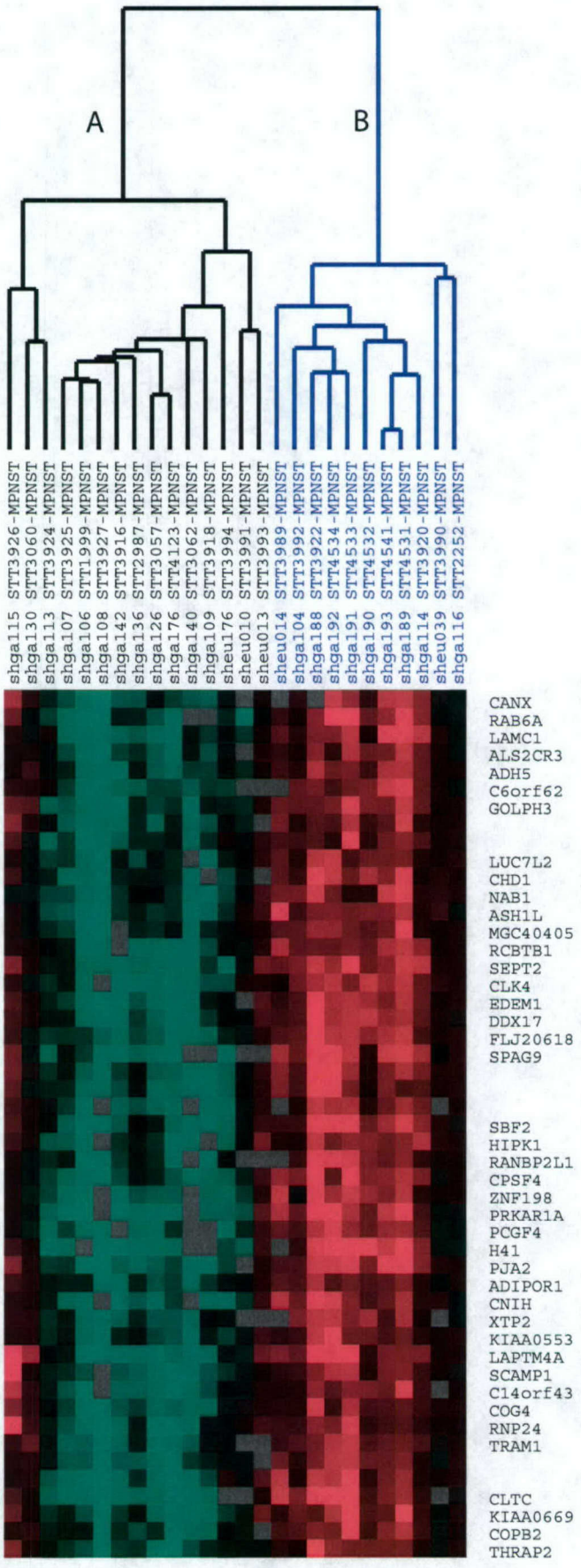
A
B
shga115 STT3926-MPNST
shga130 STT3060-MPNST
shga113 STT3924-MPNST
shga107 STT3925-MPNST
shga106 STT1999-MPNST
shga108 STT3927-MPNST
shga142 STT3916-MPNST
shga136 STT2987-MPNST
shga126 STT3057-MPNST
shga176 STT4123-MPNST
shga140 STT3062-MPNST
shga109 STT3918-MPNST
sheu176 STT3994-MPNST
sheu010 STT3991-MPNST
sheu013 STT3993-MPNST
sheu014 STT3989-MPNST
shga104 STT3992-MPNST
shga188 STT3922-MPNST
shga192 STT4534-MPNST
shga191 STT4533-MPNST
shga190 STT4532-MPNST
shga193 STT4541-MPNST
shga189 STT4531-MPNST
shga114 STT3920-MPNST
sheu039 STT3990-MPNST
shga116 STT2252-MPNST
CANX
RAB6A
LAMC1
ALS2CR3
ADH5
C6orf62
GOLPH3
LUC7L2
CHD1
NAB1
ASH1L
MGC40405
RCBTB1
SEPT2
CLK4
EDEM1
DDX17
FLJ20618
SPAG9
SBF2
HIPK1
RANBP2L1
CPSF4
ZNF198
PRKAR1A
PCGF4
H41
PJA2
ADIPOR1
CNIH
XTP2
KIAA0553
LAPTM4A
SCAMP1
C14orf43
COG4
RNP24
TRAM1
CLTC
KIAA0669
COPB2
THRAP2

Figure 5

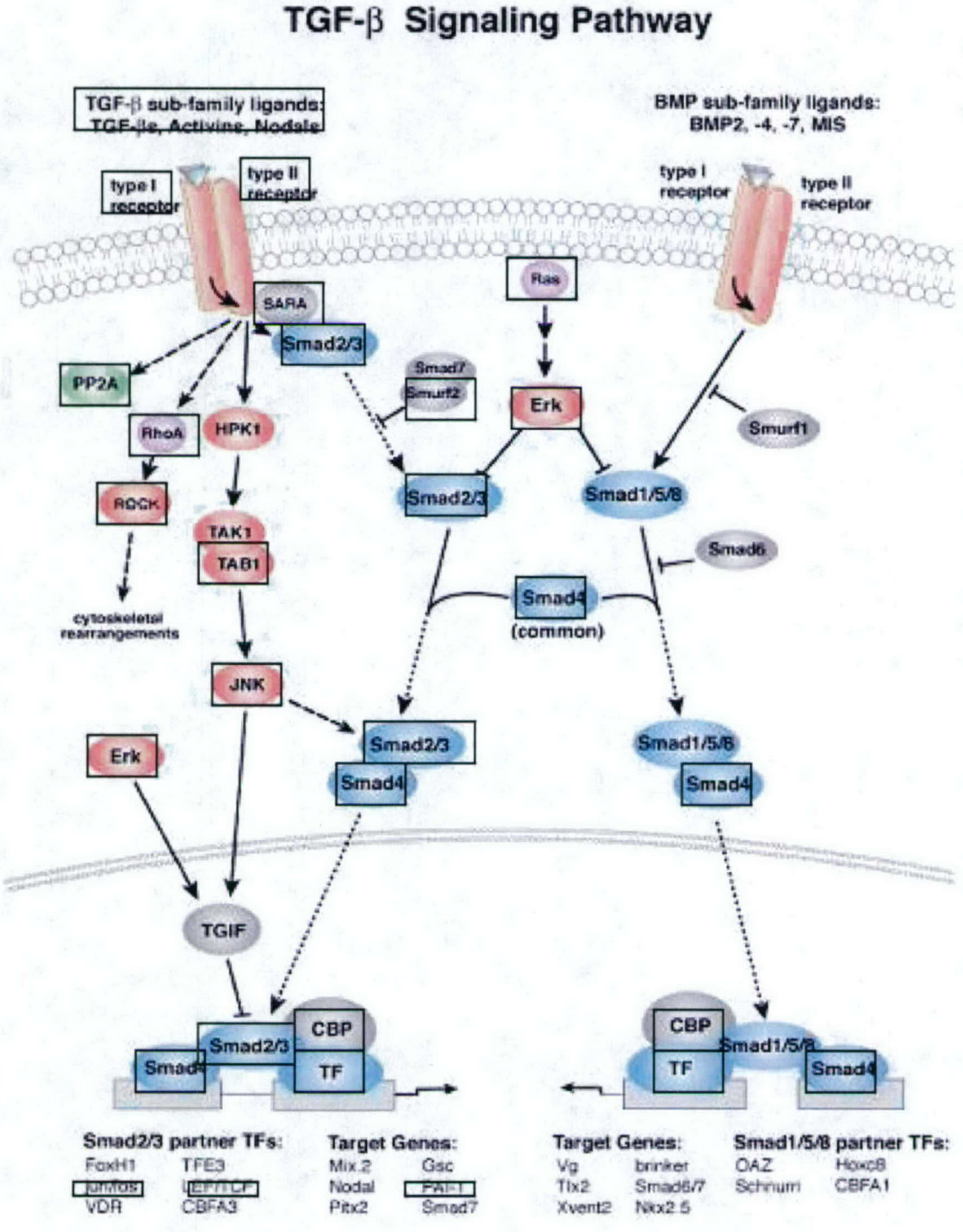
TGF-β Signaling Pathway
TGF-β sub-family ligands:
TGF-βs, Activins, Nodals
BMP sub-family ligands:
BMP2, -4, -7, MIS
type I receptor
type II receptor
type I receptor
type II receptor
SARA
Smad2/3
Ras
Smad7
Smurf2
Erk
Smurf1
PP2A
RhoA
HPK1
ROCK
TAK1
TAB1
Smad2/3
Smad1/5/8
Smad6
Smad4
(common)
cytoskeletal rearrangements
JNK
Smad2/3
Smad4
Smad1/5/8
Smad4
Erk
TGIF
CBP
Smad2/3
Smad4
TF
CBP
Smad1/5/8
Smad4
TF
Smad2/3 partner TFs:
FoxH1
TFE3
junfos
LEF1/TCF
VDR
CBFA3
Target Genes:
Mix.2
Gsc
Nodal
PAI-1
Pitx2
Smad7
Target Genes:
Vg
brinker
Tlx2
Smad6/7
Xvent2
Nkx2.5
Smad1/5/8 partner TFs:
OAZ
Hoxc8
Schnurri
CBFA1

Figure 6

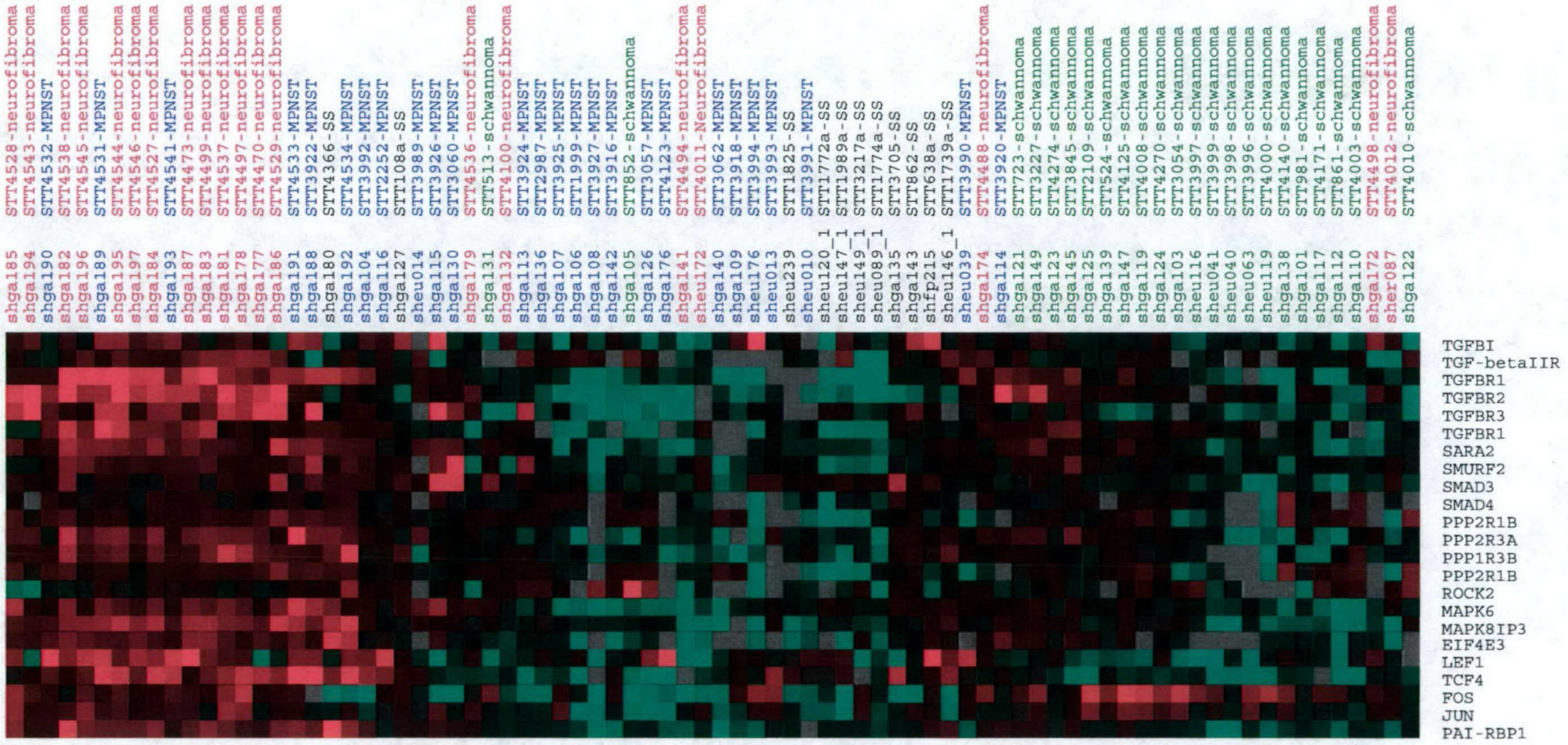
STT4528-neurofibroma
STT4543-neurofibroma
STT4532-MPNST
STT4538-neurofibroma
STT4545-neurofibroma
STT4531-MPNST
STT4544-neurofibroma
STT4546-neurofibroma
STT4527-neurofibroma
STT4541-MPNST
STT4473-neurofibroma
STT4499-neurofibroma
STT4537-neurofibroma
STT4497-neurofibroma
STT4470-neurofibroma
STT4529-neurofibroma
STT4533-MPNST
STT3922-MPNST
STT4366-SS
STT4534-MPNST
STT3992-MPNST
STT2252-MPNST
STT108a-SS
STT3989-MPNST
STT3926-MPNST
STT3060-MPNST
STT4536-neurofibroma
STT513-schwannoma
STT4100-neurofibroma
STT3924-MPNST
STT2987-MPNST
STT3925-MPNST
STT1999-MPNST
STT3927-MPNST
STT3916-MPNST
STT852-schwannoma
STT3057-MPNST
STT4123-MPNST
STT4494-neurofibroma
STT4011-Neurofibroma
STT3062-MPNST
STT3918-MPNST
STT3994-MPNST
STT3993-MPNST
STT1825-SS
STT3991-MPNST
STT1772a-SS
STT1989a-SS
STT3217a-SS
STT1774a-SS
STT3705-SS
STT862-SS
STT638a-SS
STT1739a-SS
STT3990-MPNST
STT4488-neurofibroma
STT3920-MPNST
STT723-schwannoma
STT3227-schwannoma
STT4274-schwannoma
STT3845-schwannoma
STT2109-schwannoma
STT524-schwannoma
STT4125-schwannoma
STT4008-schwannoma
STT4270-schwannoma
STT3054-schwannoma
STT3997-schwannoma
STT3999-schwannoma
STT3998-schwannoma
STT3996-schwannoma
STT4000-schwannoma
STT4140-schwannoma
STT981-schwannoma
STT4171-schwannoma
STT861-schwannoma
STT4003-schwannoma
STT4498-neurofibroma
STT4012-neurofibroma
STT4010-schwannoma
shga185
shga194
shga190
shga182
shga196
shga189
shga195
shga197
shga184
shga193
shga187
shga183
shga181
shga178
shga177
shga186
shga191
shga188
shga180
shga192
shga104
shga116
shga127
sheu014
shga115
shga130
shga179
shga131
shga132
shga113
shga136
shga107
shga106
shga108
shga142
shga105
shga126
shga176
shga141
sheu172
shga140
shga109
sheu176
sheu013
sheu239
sheu010
sheu120_1
sheu147_1
sheu149_1
sheu089_1
shga135
shga143
shfp215
sheu146_1
sheu039
shga174
shga114
shga121
shga149
shga123
shga145
shga125
shga139
shga147
shga119
shga124
shga103
sheu116
sheu041
sheu040
sheu063
sheu119
shga138
shga101
shga117
shga112
shga110
shga172
sher087
shga122
TGFBI
TGF-betaIIR
TGFBR1
TGFBR2
TGFBR3
TGFBR1
SARA2
SMURF2
SMAD3
SMAD4
PPP2R1B
PPP2R3A
PPP1R3B
PPP2R1B
ROCK2
MAPK6
MAPK8IP3
EIF4E3
LEF1
TCF4
FOS
JUN
PAI-RBP1

Figure 7

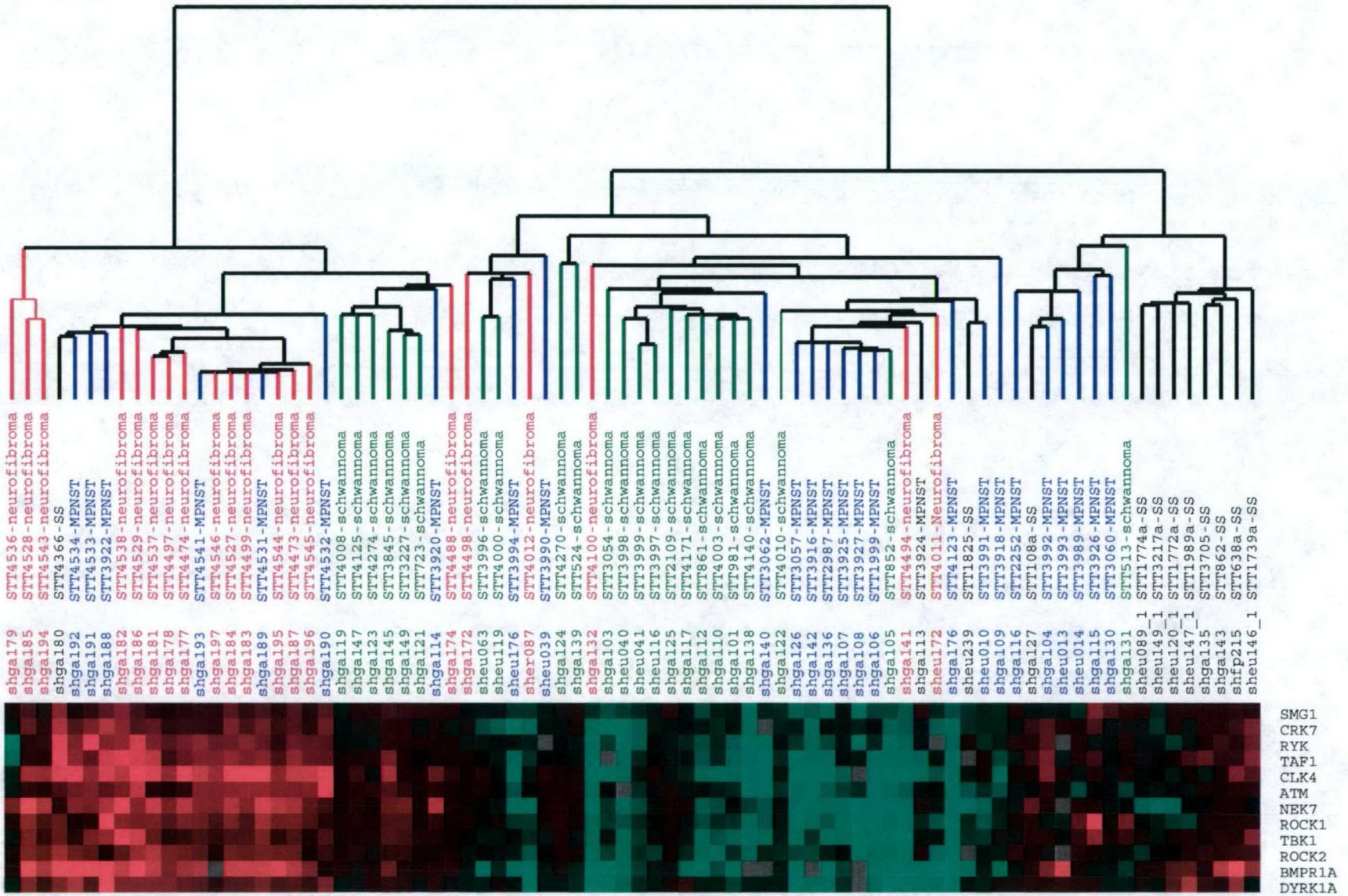
STT4536-neurofibroma
STT4528-neurofibroma
STT4543-neurofibroma
STT4366-SS
STT4534-MPNST
STT4533-MPNST
STT3922-MPNST
STT4538-neurofibroma
STT4529-neurofibroma
STT4537-neurofibroma
STT4497-neurofibroma
STT4474-neurofibroma
STT4541-MPNST
STT4546-neurofibroma
STT4527-neurofibroma
STT4499-neurofibroma
STT4531-MPNST
STT4544-neurofibroma
STT4473-neurofibroma
STT4545-neurofibroma
STT4532-MPNST
STT4008-schwannoma
STT4125-schwannoma
STT4274-schwannoma
STT3845-schwannoma
STT3227-schwannoma
STT723-schwannoma
STT3920-MPNST
STT4488-neurofibroma
STT4498-neurofibroma
STT3996-schwannoma
STT4000-schwannoma
STT3994-MPNST
STT4012-neurofibroma
STT3990-MPNST
STT4270-schwannoma
STT524-schwannoma
STT4100-neurofibroma
STT3054-schwannoma
STT3998-schwannoma
STT3999-schwannoma
STT3997-schwannoma
STT2109-schwannoma
STT4171-schwannoma
STT861-schwannoma
STT4003-schwannoma
STT981-schwannoma
STT4140-schwannoma
STT3062-MPNST
STT4010-schwannoma
STT3057-MPNST
STT3916-MPNST
STT2987-MPNST
STT3925-MPNST
STT3927-MPNST
STT1999-MPNST
STT852-schwannoma
STT4494-neurofibroma
STT3924-MPNST
STT4011-Neurofibroma
STT4123-MPNST
STT1825-SS
STT3991-MPNST
STT3918-MPNST
STT2252-MPNST
STT1108a-SS
STT3992-MPNST
STT3993-MPNST
STT3989-MPNST
STT3926-MPNST
STT3060-MPNST
STT513-schwannoma
STT1774a-SS
STT3217a-SS
STT1772a-SS
STT1989a-SS
STT3705-SS
STT862-SS
STT638a-SS
STT1739a-SS
shga179
shga185
shga194
shga180
shga192
shga191
shga188
shga182
shga186
shga181
shga178
shga177
shga193
shga197
shga184
shga183
shga189
shga195
shga187
shga196
shga190
shga119
shga147
shga123
shga145
shga149
shga121
shga114
shga174
shga172
sheu063
sheu119
sheu176
sher087
sheu039
shga124
shga139
shga132
shga103
sheu040
sheu041
sheu116
shga125
shga117
shga112
shga110
shga101
shga138
shga140
shga122
shga126
shga142
shga136
shga107
shga108
shga106
shga105
shga141
shga113
sheu172
shga176
sheu239
sheu010
shga109
shga116
shga127
shga104
sheu013
sheu014
shga115
shga130
shga131
sheu089_1
sheu149_1
sheu120_1
sheu147_1
shga135
shga143
shfp215
sheu146_1
SMG1
CRK7
RYK
TAF1
CLK4
ATM
NEK7
ROCK1
TBK1
ROCK2
BMPR1A
DYRK1A

Figure 8

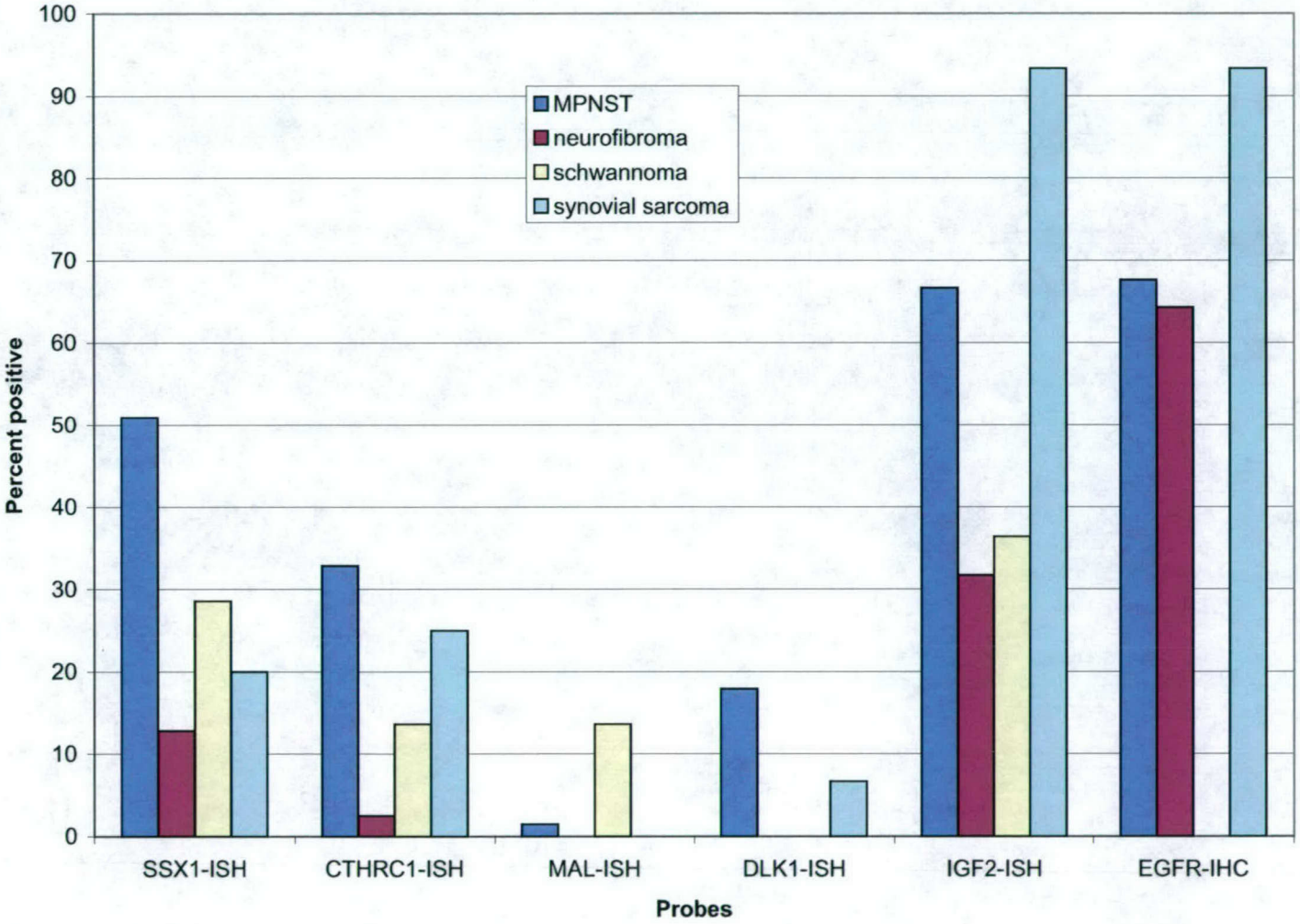
100
90
80
70
60
50
40
30
20
10
0
Percent positive
MPNST
neurofibroma
schwannoma
synovial sarcoma
SSX1-ISH
CTHRC1-ISH
MAL-ISH
DLK1-ISH
IGF2-ISH
EGFR-IHC
Probes

Figure 9

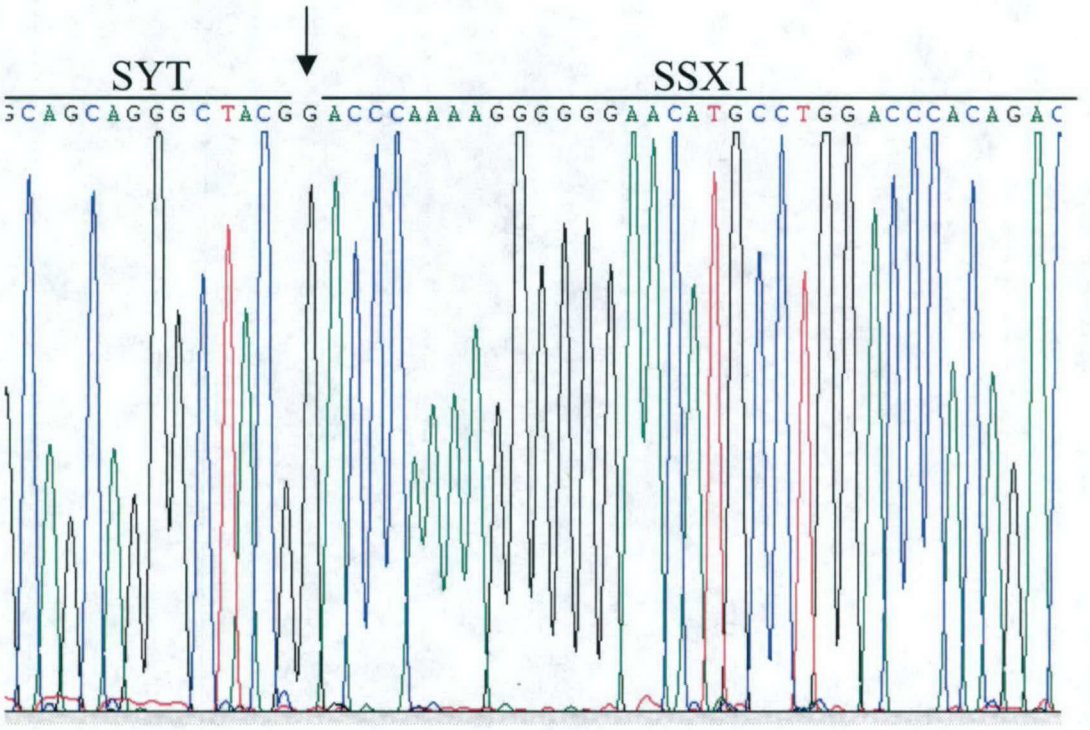
SYT
SSX1
GCAGCAGGGCTACGGACCCAAAAGGGGGGAACATGCCTGGACCCACAGAC

LEGENDS FOR FIGURES

Figure 1
Unsupervised hierarchical cluster analysis of gene expression profiles of 80 nerve sheath tumors using 4137 genes.

Figure 2
Overview of expression pattern of the 4137 genes used for hierarchical cluster analysis. Each row represents the relative levels of expression for a single gene, centered at the geometric mean of its expression levels across the 36 samples. Each column shows the expression levels for a single sample. The red or green color indicates high or low expression, respectively.

Figure 3
Unsupervised hierarchical cluster analysis of gene expression profiles of 26 MPNSTs and 20 neurofibromas.

Figure 4
Unsupervised hierarchical cluster analysis of gene expression profiles of 26 MPNSTs.

Figure 5
TGFB signaling pathway genes. Genes that are highlighted by box are highly expressed in majority of neurofibromas (pathway figure is adopted from cellsignal.com).

Figure 6
Differential gene expression pattern showing the selected genes that are associated with TGFB signaling pathway.

Figure 7
Unsupervised hierarchical cluster analysis of gene expression profiles of 80 nerve sheath tumors using the 409 human kinase gene list that we compiled. A subset of kinase genes that are highly expressed in most of the neurofibromas are shown.

Figure 8
Graphical representation of percentage of positive staining for ISH and IHC probes on TA-138.

Figure 9
DNA sequence electropherogram showing the fusion of SYT and SSX1 genes in a MPNST case.

Table 1a

Gene Symbol	Gene name	Unigene No.	Score(d)	Fold Change
ZIC1	Zic family member 1 (odd-paired homolog, Drosophila)	Hs.41154	3.4898	4.05622
PCOLCE	Procollagen C-endopeptidase enhancer	Hs.202097	3.0421	2.41187
ADNP	Activity-dependent neuroprotector	Hs.293736	2.9474	2.83948
PYCR1	Pyrroline-5-carboxylate reductase 1	Hs.458332	2.9011	2.69205
CTHRC1	Collagen triple helix repeat containing 1	Hs.405614	2.7255	3.20481
LRRC17	Leucine rich repeat containing 17	Hs.552582	2.6633	2.16789
RGS4	Regulator of G-protein signalling 4	Hs.386726	2.6287	2.47910
SEMA3A	Sema domain, immunoglobulin domain (Ig)	Hs.252451	2.6138	1.92881
CDC25C	Cell division cycle 25C	Hs.656	2.5784	2.13304
EIF2B3	Eukaryotic translation initiation factor 2B	Hs.533549	2.5750	2.68014
DNM1	Dynamin 1	Hs.522413	2.5360	2.21243
OTX2	Orthodenticle homolog 2 (Drosophila)	Hs.288655	2.5129	1.71642
ELN	Elastin	Hs.252418	2.5071	3.25434
TTK	TTK protein kinase	Hs.169840	2.4902	1.99223
TPX2	TPX2, microtubule-associated protein homolog	Hs.244580	2.4782	2.21512
ASAM	Adipocyte-specific adhesion molecule	Hs.504187	2.4567	2.44982
INA	Internexin neuronal intermediate filament protein, alpha	Hs.500916	2.4295	2.76223
MYBL2	V-myb myeloblastosis viral oncogene homolog (avian)-like 2	Hs.179718	2.4186	2.32711
THBS4	Thrombospondin 4	Hs.211426	2.4080	3.43319
CAMK4	Calcium/calmodulin-dependent protein kinase IV	Hs.220629	2.4001	2.99391
OSBPL6	Oxysterol binding protein-like 6	Hs.318775	2.3973	1.89798
FGFR1	Fibroblast growth factor receptor 1	Hs.549034	2.3610	1.88302
PLEKHH2	Pleckstrin homology domain containing	Hs.164162	2.3434	2.13871
CDC6	CDC6 cell division cycle 6 homolog (S. cerevisiae)	Hs.405958	2.3428	2.79805
CENPF	Centromere protein F, 350/400ka (mitosin)	Hs.497741	2.3195	2.35200
MSX1	Msh homeo box homolog 1 (Drosophila)	Hs.424414	2.3012	1.60015
PTK7	PTK7 protein tyrosine kinase 7	Hs.90572	2.2954	2.21401
FLJ25416	Hypothetical protein FLJ25416	Hs.165607	2.2674	1.88447
RGS4	Regulator of G-protein signalling 4	Hs.386726	2.2602	2.15564
LRRC17	Leucine rich repeat containing 17	Hs.552582	2.2538	2.28211
PHTF2	Putative homeodomain transcription factor 2	Hs.203965	2.2534	2.03853
ADAM12	A disintegrin and metalloproteinase domain 12 (meltrin alpha)	Hs.386283	2.2449	5.12345
TRPA1	Transient receptor potential cation channel	Hs.137674	2.2396	2.41367
C20orf129	Chromosome 20 open reading frame 129	Hs.472716	2.2355	1.83122
EGFR	Epidermal growth factor receptor	Hs.488293	2.2275	2.52289
GATA3	GATA binding protein 3	Hs.524134	2.2273	1.82224
EGFR	Epidermal growth factor receptor	Hs.488293	2.2171	2.52895
ALPK2	Alpha-kinase 2	Hs.388674	2.2017	3.53060
CRABP1	Cellular retinoic acid binding protein 1	Hs.346950	2.1888	1.65871
UBE2C	Ubiquitin-conjugating enzyme E2C	Hs.93002	2.1809	1.99864
MEST	Mesoderm specific transcript homolog (mouse)	Hs.270978	2.1790	2.49519
DLG7	Discs, large homolog 7 (Drosophila)	Hs.77695	2.1737	1.87322
COL11A2	Collagen, type XI, alpha 2	Hs.390171	2.1636	2.20879
ADAMTS3	A disintegrin-like and metalloprotease	Hs.151435	2.1608	2.28252

Table 1b

Gene	Gene Name	Unigene No.	Score(d)	Fold Change
INPP5F	Inositol polyphosphate-5-phosphatase F	Hs.369755	4.6284	7.92009
PALMD	Palmdelphin	Hs.483993	4.2910	7.02622
TFPI	Tissue factor pathway inhibitor	Hs.516578	4.2738	3.76718
P2RY14	Purinergic receptor P2Y, G-protein coupled, 14	Hs.2465	4.1892	4.90736
BCHE	Butyrylcholinesterase	Hs.420483	4.0829	9.96892
ABCG2	ATP-binding cassette, sub-family G (WHITE), member 2	Hs.480218	3.9754	4.16427
TGFBR2	Transforming growth factor, beta receptor II (70/80kDa)	Hs.82028	3.7045	3.99231
TM4SF10	Transmembrane 4 superfamily member 10	Hs.8769	3.6447	4.25401
PDE8A	Phosphodiesterase 8A	Hs.9333	3.6164	4.44809
FLJ13912	Hypothetical protein FLJ13912	Hs.47125	3.5851	6.32244
CAV1	Caveolin 1, caveolae protein, 22kDa	Hs.74034	3.5740	4.57819
OPHN1	Oligophrenin 1	Hs.128824	3.5553	3.29443
IGSF11	Immunoglobulin superfamily, member 11	Hs.112873	3.5348	3.55520
ADH1B	Alcohol dehydrogenase IB (class I), beta polypeptide	Hs.4	3.5335	3.74482
DSCR1L1	Down syndrome critical region gene 1-like 1	Hs.440168	3.4854	3.08548
DOC1	Downregulated in ovarian cancer 1	Hs.104672	3.4515	5.40770
LUM	Lumican	Hs.406475	3.4351	3.14451
SIAT10	ST3 beta-galactoside alpha-2,3-sialyltransferase 6	Hs.148716	3.4307	3.66366
ELOVL2	Elongation of very long chain fatty acids	Hs.408557	3.4304	4.99638
AKR1C3	Aldo-keto reductase family 1, member C3	Hs.78183	3.3736	3.46594
AD031	AD031 protein	Hs.44004	3.3448	3.27860
LAMA4	Laminin, alpha 4	Hs.213861	3.3324	4.14941
GPA33	Glycoprotein A33 (transmembrane)	Hs.437229	3.3321	4.12233
PRO2949	Hypothetical protein PRO2949	Hs.391480	3.3280	5.52045
GNG2	Guanine nucleotide binding protein (G protein), gamma 2	Hs.187772	3.3146	7.55056
TM4SF1	Transmembrane 4 superfamily member 1	Hs.351316	3.3010	2.78933
PDGFRL	Platelet-derived growth factor receptor-like	Hs.458573	3.2948	2.96099
ARGBP2	Arg/Abl-interacting protein ArgBP2	Hs.481342	3.2717	2.87008
LUM	Lumican	Hs.406475	3.2634	2.74251
LAMA4	Laminin, alpha 4	Hs.213861	3.2500	3.00714
SOX5	SRY (sex determining region Y)-box 5	Hs.505007	3.2385	4.05959
EDNRB	Endothelin receptor type B	Hs.82002	3.2348	3.59887
CIT	Citron (rho-interacting, serine/threonine kinase 21)	Hs.119594	3.2231	3.19637
ADAMTS1	A disintegrin-like and metalloprotease with thrombospondin type 1 motif, 1	Hs.534115	3.2064	3.05966
IGF1	Insulin-like growth factor 1 (somatomedin C)	Hs.160562	3.2042	3.64754
GAB1	GRB2-associated binding protein 1	Hs.80720	3.2026	3.58551
CAV2	Caveolin 2	Hs.212332	3.2012	2.83580
FLJ20481	Hypothetical protein FLJ20481	Hs.460857	3.1960	3.19566
DSCR1L1	Down syndrome critical region gene 1-like 1	Hs.440168	3.1946	2.75723
CMAH	Cytidine monophosphate-N-acetylneuraminic acid hydroxylase	Hs.484918	3.1930	2.69363
AP1S2	Adaptor-related protein complex 1, sigma 2 subunit	Hs.121592	3.1723	3.29826
TMEM30A	Transmembrane protein 30A	Hs.108530	3.1643	3.47552
MCTP1	Multiple C2-domains with two transmembrane regions 1	Hs.209095	3.1191	2.92832
GAB1	GRB2-associated binding protein 1	Hs.80720	3.1063	3.59259
SASH1	SAM and SH3 domain containing 1	Hs.193133	3.1052	3.97481

Table 1c

Gene Symbol	Gene Name	Unigene No.	Score(d)	Fold Change
SERPINA5	Serine (or cysteine) proteinase inhibitor,	Hs.510334	5.6708	10.93367
APOC2	Apolipoprotein C-II	Hs.75615	5.0271	5.14792
CLU	Clusterin	Hs.436657	4.7870	4.34179
BAIAP2	BAI1-associated protein 2	Hs.128316	4.7690	7.96437
MAL	Mal, T-cell differentiation protein	Hs.80395	4.7362	6.48818
HLA-DRB5	Major histocompatibility complex, class II, DR beta 4	Hs.534322	4.5282	3.39913
APCS	Amyloid P component, serum	Hs.507080	4.4549	3.82308
L1CAM	L1 cell adhesion molecule	Hs.522818	4.4435	5.24206
PLXNB3	Plexin B3	Hs.380742	4.3471	3.98056
RPESP	RPE-spondin	Hs.439040	4.3299	4.54979
CTNNAL1	Catenin (cadherin-associated protein), alpha-like 1	Hs.58488	4.2947	3.50911
SOX10	SRY (sex determining region Y)-box 10	Hs.376984	4.2731	3.16337
SUPT3H	Suppressor of Ty 3 homolog (S. cerevisiae)	Hs.368325	4.2635	4.43046
RAB20	RAB20, member RAS oncogene family	Hs.508720	4.2536	3.51322
ANK3	Ankyrin 3, node of Ranvier (ankyrin G)	Hs.499725	4.2231	3.63067
HLA-DRB1	Major histocompatibility complex, class II, DR beta 4	Hs.520049	4.1804	3.13547
MGC52010	Hypothetical protein MGC52010	Hs.526933	4.1602	3.42691
APOC1	Apolipoprotein C-I	Hs.110675	4.1292	3.40753
ALOX5AP	Arachidonate 5-lipoxygenase-activating protein	Hs.507658	4.0837	3.65825
RPESP	RPE-spondin	Hs.439040	4.0668	3.83018
PCOLN3	Procollagen (type III) N-endopeptidase	Hs.461777	4.0488	4.81950
MT1K	Metallothionein 1K	Hs.188518	4.0205	4.66846
TMOD2	Tropomodulin 2 (neuronal)	Hs.513734	4.0050	3.61435
HLA-DRB1	Major histocompatibility complex, class II, DR beta 4	Hs.520049	3.9940	3.22295
FLJ14525	Hypothetical protein FLJ14525	Hs.520494	3.9940	3.21829
SIAT7B	ST6 (alpha-N-acetyl-neuraminyl-2,3-beta-galactosyl-1,3)	Hs.281434	3.9792	3.06313
CD37	CD37 antigen	Hs.166556	3.9547	2.92279
VMD2	Vitelliform macular dystrophy (Best disease, bestrophin)	Hs.132319	3.9417	3.04403
CDH1	Cadherin 1, type 1, E-cadherin (epithelial)	Hs.461086	3.9254	3.50404
MARCH-II	Membrane-associated ring finger (C3HC4) 2	Hs.445113	3.9188	2.78786
SLC2A5	Solute carrier family 2	Hs.530003	3.9176	3.38609
DHRS3	Dehydrogenase/reductase (SDR family) member 3	Hs.289347	3.8958	3.42356
SORL1	Sortilin-related receptor, L(DLR class) A repeats-containing	Hs.368592	3.8794	2.90360
RASSF4	Ras association (RalGDS/AF-6) domain family 4	Hs.522895	3.7992	3.08389
MT1E	Metallothionein 1E (functional)	Hs.534330	3.7874	3.27153
DDR1	Discoidin domain receptor family, member 1	Hs.520004	3.7781	2.49268
ACTA2	Actin, alpha 2, smooth muscle, aorta	Hs.500483	3.7606	2.67650
SYN3	Synapsin III	Hs.125878	3.7586	3.12328
MBP	Myelin basic protein	Hs.501262	3.7532	4.30273
HLA-DOA	Major histocompatibility complex, class II, DO alpha	Hs.351874	3.7201	3.06062
LILRB4	Leukocyte immunoglobulin-like receptor,	Hs.67846	3.6924	2.93889
SPTBN1	Spectrin, beta, non-erythrocytic 1	Hs.503178	3.6637	3.16527
MYO1F	Myosin IF	Hs.408451	3.6553	2.90615
ANK3	Ankyrin 3, node of Ranvier (ankyrin G)	Hs.499725	3.6489	2.97184
C1QB	Complement component 1, q subcomponent, beta polypeptide	Hs.8986	3.6361	2.17454
D15Wsu75e	DNA segment, Chr 15, Wayne State University 75, expressed	Hs.335274	3.6339	3.63507

Table 1d

Gene Symbol	Gene Name	Unigen NO.	Score(d)	Fold Change
ZIC2	Zic family member 2 (odd-paired homolog, Drosophila)	Hs.369063	4.4528	46.2745
SSX1	Synovial sarcoma, X breakpoint 1	Hs.434142	3.7107	12.2965
EFNB3	Ephrin-B3	Hs.26988	3.5988	9.99709
CRABP2	Cellular retinoic acid binding protein 2	Hs.405662	2.8273	5.45803
FZD1	Frizzled homolog 1 (Drosophila)	Hs.94234	2.6957	5.78501
RIPK4	Receptor-interacting serine-threonine kinase 4	Hs.517310	2.6641	4.44980
MSX2	Msh homeo box homolog 2 (Drosophila)	Hs.89404	2.6204	12.1827
ENC1	Ectodermal-neural cortex (with BTB-like domain)	Hs.104925	2.6188	5.93634
EPHA4	EPH receptor A4	Hs.371218	2.6173	6.25807
SHANK2	SH3 and multiple ankyrin repeat domains 2	Hs.268726	2.5947	5.81334
CXXC4	CXXC finger 4	Hs.12248	2.5920	5.47491
CRABP2	Cellular retinoic acid binding protein 2	Hs.405662	2.5899	4.89089
ENC1	Ectodermal-neural cortex (with BTB-like domain)	Hs.104925	2.5667	7.04168
COL2A1	Collagen, type II, alpha 1	Hs.408182	2.5090	3.84286
FZD1	Frizzled homolog 1 (Drosophila)	Hs.94234	2.4909	6.32802
FOXD1	Forkhead box D1	Hs.519385	2.4443	5.22823
CLUL1	Clusterin-like 1 (retinal)	Hs.274959	2.4362	5.50355
CRABP1	Cellular retinoic acid binding protein 1	Hs.346950	2.4248	5.97855
APLP1	Amyloid beta (A4) precursor-like protein 1	Hs.74565	2.4098	4.65201
KCNQ1OT1	Potassium voltage-gated channel, KQT-like subfamily, member 1	Hs.95162	2.3474	3.62065
FOXF2	Forkhead box F2	Hs.484423	2.3446	6.70823
MEIS1	Meis1, myeloid ecotropic viral integration site 1 homolog (mouse)	Hs.526754	2.3113	4.03120
HUNK	Hormonally upregulated Neu-associated kinase	Hs.109437	2.3047	4.11739
MYO9B	Myosin IXB	Hs.123198	2.2413	5.41403
IGF2	Insulin-like growth factor 2 (somatomedin A)	Hs.549043	2.2012	2.59220
KCNQ1OT1	Potassium voltage-gated channel, KQT-like subfamily, member 1	Hs.95162	2.1965	3.51236
COL27A1	Collagen, type XXVII, alpha 1	Hs.494892	2.1904	4.42386
MGC10433	Hypothetical protein MGC10433	Hs.5086	2.1827	4.31909
TUSC3	Tumor suppressor candidate 3	Hs.426324	2.1742	3.43976
FGF9	Fibroblast growth factor 9 (glia-activating factor)	Hs.111	2.1732	4.99088
SIM2	Single-minded homolog 2 (Drosophila)	Hs.146186	2.1691	6.89322
TRPS1	Trichorhinophalangeal syndrome I	Hs.253594	2.1494	5.82309
COL4A5	Collagen, type IV, alpha 5 (Alport syndrome)	Hs.369089	2.1408	4.26767
CRA	Cisplatin resistance associated	Hs.425144	2.1251	4.05153
TUSC3	Tumor suppressor candidate 3	Hs.426324	2.1175	3.05891
TACSTD1	Tumor-associated calcium signal transducer 1	Hs.692	2.1025	16.395
CRA	Cisplatin resistance associated	Hs.425144	2.1002	3.72197
GLI2	GLI-Kruppel family member GLI2	Hs.111867	2.0436	3.78270
ROBO1	Roundabout, axon guidance receptor, homolog 1 (Drosophila)	Hs.13640	2.0368	2.84573
BEX2	Brain expressed X-linked 2	Hs.398989	2.0271	3.89705
HSRG1	MON1 homolog B (yeast)	Hs.513743	2.0191	9.39712
CPA3	Carboxypeptidase A3 (mast cell)	Hs.646	2.0184	5.52722
TACSTD1	Tumor-associated calcium signal transducer 1	Hs.692	2.0175	18.284
TLE1	Transducin-like enhancer of split 1 (E(sp1) homolog, Drosophila)	Hs.197320	2.0157	3.88361
TLE4	Transducin-like enhancer of split 4 (E(sp1) homolog, Drosophila)	Hs.444213	2.0091	3.82059
LOC492304	Putative insulin-like growth factor II associated protein	Hs.523414	2.0082	2.20428

Table 2a

Gene Symbol	Gene Name	Unigene No	Score(d)	Fold Change
CRABP1	Cellular retinoic acid binding protein 1	Hs.346950	2.81064	12.32367
DLX4	Distal-less homeobox 4	Hs.172648	2.70473	6.86763
DKFZp762E1312	Hypothetical protein DKFZp762E1312	Hs.532968	2.55278	3.67592
UBE2C	Ubiquitin-conjugating enzyme E2C	Hs.93002	2.49854	3.35699
CPA3	Carboxypeptidase A3 (mast cell)	Hs.646	2.48257	6.82227
COL11A2	Collagen, type XI, alpha 2	Hs.390171	2.45024	9.75650
DLX4	Distal-less homeobox 4	Hs.172648	2.43615	4.96286
NEK2	NIMA (never in mitosis gene a)-related kinase 2	Hs.153704	2.41043	2.72443
PYCR1	Pyrroline-5-carboxylate reductase 1	Hs.458332	2.39372	3.31893
MFAP2	Microfibrillar-associated protein 2	Hs.389137	2.38870	5.11839
TOP2A	Topoisomerase (DNA) II alpha 170kDa	Hs.156346	2.37510	3.21511
RASL11B	RAS-like, family 11, member B	Hs.8035	2.24331	10.25158
NUSAP1	Nucleolar and spindle associated protein 1	Hs.511093	2.23432	3.90908
HBZ	Hemoglobin, zeta	Hs.449632	2.19165	2.50073
OTX2	Orthodenticle homolog 2 (Drosophila)	Hs.288655	2.16363	7.94141
TPX2	TPX2, microtubule-associated protein homolog (Xenopus laevis)	Hs.244580	2.12050	2.73443
GLI2	GLI-Kruppel family member GLI2	Hs.111867	2.06957	3.08229
ADNP	Activity-dependent neuroprotector	Hs.293736	2.05931	3.32727
LOC492304	Putative insulin-like growth factor II associated protein	Hs.523414	1.97549	4.85270
CENPF	Centromere protein F, 350/400ka (mitosin)	Hs.497741	1.97359	2.84956
UBE2C	Ubiquitin-conjugating enzyme E2C	Hs.93002	1.95085	2.66466
SLC6A15	Solute carrier family 6, member 15	Hs.44424	1.94491	2.91352

Table 2b

Gene Symbol	Gene Name	Unigene No	Score(d)	Fold Change
EPHA4	EPH receptor A4	Hs.371218	3.2445	6.15098
CDH2	Cadherin 2, type 1, N-cadherin (neuronal)	Hs.464829	2.9982	3.49727
LOC152485	Hypothetical protein LOC152485	Hs.133916	2.9470	4.24594
CRABP1	Cellular retinoic acid binding protein 1	Hs.346950	2.9408	20.35889
RGS4	Regulator of G-protein signalling 4	Hs.386726	2.7262	5.10985
STXBP6	Syntaxin binding protein 6 (amisyn)	Hs.508958	2.6584	5.43809
LOC492304	Putative insulin-like growth factor II associated protein	Hs.523414	2.6566	5.26394
STC1	Stanniocalcin 1	Hs.25590	2.6534	2.96513
MFAP2	Microfibrillar-associated protein 2	Hs.389137	2.6330	6.19999
GLI2	GLI-Kruppel family member GLI2	Hs.111867	2.6275	4.48209
FABP4	Fatty acid binding protein 4, adipocyte	Hs.391561	2.6188	4.59194
ENC1	Ectodermal-neural cortex (with BTB-like domain)	Hs.104925	2.5821	6.14182
NETO2	Neuropilin (NRP) and tolloid (TLL)-like 2	Hs.444046	2.5438	2.99612
LOC492304	Putative insulin-like growth factor II associated protein	Hs.523414	2.5331	18.58836
NEFL	Neurofilament, light polypeptide 68kDa	Hs.521461	2.5241	10.58529
UBE2C	Ubiquitin-conjugating enzyme E2C	Hs.93002	2.4920	4.80146
POSTN	Periostin, osteoblast specific factor	Hs.136348	2.4494	10.07362
MYBL1	V-myb myeloblastosis viral oncogene homolog (avian)-like 1	Hs.445898	2.4333	2.28412
LPHN2	Latrophilin 2	Hs.24212	2.4276	3.40050
PCSK5	Proprotein convertase subtilisin/kexin type 5	Hs.368542	2.3965	5.98308
PBX1	Pre-B-cell leukemia transcription factor 1	Hs.493096	2.3917	2.71545
IGF2	Insulin-like growth factor 2 (somatomedin A)	Hs.549043	2.3868	10.45371
SEMA3A	Sema domain, immunoglobulin domain (Ig),	Hs.252451	2.3769	3.34582
PYCR1	Pyrroline-5-carboxylate reductase 1	Hs.458332	2.3263	2.60545
MGP	Matrix Gla protein	Hs.365706	2.3232	6.54398
STRA6	Stimulated by retinoic acid gene 6 homolog (mouse)	Hs.24553	2.3224	5.62322
DSP	Desmoplakin	Hs.519873	2.3155	3.52630
MSX1	Msh homeo box homolog 1 (Drosophila)	Hs.424414	2.2927	4.44980
KCNQ1OT1	Potassium voltage-gated channel, KQT-like subfamily, member 1	Hs.95162	2.2770	3.54560
FRAS1	Fraser syndrome 1	Hs.369448	2.2568	2.74847
PBX1	Pre-B-cell leukemia transcription factor 1	Hs.493096	2.2516	3.89808
REN	Renin	Hs.3210	2.2319	2.76857
RAB27B	RAB27B, member RAS oncogene family	Hs.25318	2.2281	5.21021
LOC492304	Putative insulin-like growth factor II associated protein	Hs.523414	2.2084	5.93568
RASL11B	RAS-like, family 11, member B	Hs.8035	2.1825	19.95145
ROBO1	Roundabout, axon guidance receptor, homolog 1 (Drosophila)	Hs.13640	2.1769	3.25809
INHBA	Inhibin, beta A (activin A, activin AB alpha polypeptide)	Hs.28792	2.1415	3.74975
ROBO1	Roundabout, axon guidance receptor, homolog 1 (Drosophila)	Hs.13640	2.1380	2.48258
FRAS1	Fraser syndrome 1	Hs.369448	2.1309	2.94461
CRABP2	Cellular retinoic acid binding protein 2	Hs.405662	2.1210	6.89519
MFAP5	Microfibrillar associated protein 5	Hs.512842	2.0982	6.86064
SLPI	Secretory leukocyte protease inhibitor (antileukoproteinase)	Hs.517070	2.0847	2.57178
LRP4	Low density lipoprotein receptor-related protein 4	Hs.4930	2.0747	3.20622
CADPS	Ca2+-dependent secretion activator	Hs.127013	2.0623	3.59715

Table 2c

Gene Symbol	Gene Name	Unigene No	Score(d)	Fold Change
FLJ43172	CDNA FLJ43172 fis, clone FCBBF3007242	Hs.446660	0.6495	6.40335
TTK	TTK protein kinase	Hs.169840	0.6714	2.87463
NUSAP1	Nucleolar and spindle associated protein 1	Hs.511093	0.8408	6.28607
CYP24A1	Cytochrome P450, family 24, subfamily A,	Hs.89663	0.4718	2.63081
DLX4	Distal-less homeobox 4	Hs.172648	0.6506	6.14456
CDH11	Cadherin 11, type 2, OB-cadherin (osteoblast)	Hs.116471	0.5008	2.86453
DKFZp762E1312	Hypothetical protein DKFZp762E1312	Hs.532968	0.6904	4.41892
TM4SF13	Transmembrane 4 superfamily member 13	Hs.364544	0.7013	6.11857
HBZ	Hemoglobin, zeta	Hs.449632	0.6164	3.34762
PRKDC	Protein kinase, DNA-activated, catalytic polypeptide	Hs.491682	0.5634	2.44666
ANLN	Anillin, actin binding protein	Hs.62180	0.8083	4.36933
NEK2	NIMA (never in mitosis gene a)-related kinase 2	Hs.153704	0.6219	2.76796
TPX2	TPX2, microtubule-associated protein homolog	Hs.244580	0.9002	4.29848

LEGEND FOR TABLES

Table 1a
A partial list of genes with highest differential expression in MPNSTs according to SAM analysis.

Table 1b
A partial list of genes with highest differential expression in neurofibromas according to SAM analysis.

Table 1c
A partial list of genes with highest differential expression in schwannomas according to SAM analysis.

Table 1d
A partial list of genes with highest differential expression in synovial sarcomas according to SAM analysis.

Table 2a
A partial list of genes with highest differential expression in MPNSTs vs neurofibromas in figure 3 according to SAM analysis.

Table 2b
A partial list of genes with highest differential expression in 17 MPNSTs that clustered in branch A of **Figure** 3 compared with the rest of neurofibromas in the branch A of the cluster.

Table 2c
A partial list of genes with highest differential expression in 9 MPNSTs that clustered in branch B of **Figure** 3 compared with the rest of neurofibromas in the branch B of the cluster.

KEY RESEARCH ACCOMPLISHMENTS

1. Gene expression profiling on a large number (80 cases) on nerve sheath tumors and the related lesion synovial sarcoma

- Bioinformatical and statistical analyses.
- Identification of genes that are associated with malignant transformation.

2. Construction of tissue microarray with 200 nerve sheath lesions.
- Development of in situ hybridization probes.
- Testing antibodies by immunohistochemistry.

REPORTABLE OUTCOMES:

So far we have been in data acquisition phase and have not published any papers or abstracts.

CONCLUSIONS

In the past year we performed gene microarray analysis on a large numbers of MPNSTs, neurofibromas, schwannomas, and synovial sarcomas. In the statement above we show that we have started the significant amount of bioinformatic analysis that needs to be performed on these datasets. At the same time we have generated a tissue microarray that is already being used to test the first candidates for MPNST markers. It appears however that the MPNSTs are relatively heterogeneous and we are currently pursuing the idea that indeed at least two subtypes of MPNSTs exist as indicated by the gene microarray gene expression profiling data. From our preliminary analysis it seems that finding one marker that will positively identify all MPNSTs will be difficult and we believe that given the possible existence of subtypes of MPNSTs we will be forced to look at groups of genes that indicate malignant transformation in nerve sheath tumors and can serve as a positive marker for MPNST. At this point it should be noted that currently in histological diagnostic systems no true positive markers for MPNST exists. The markers that are described (such as S100) are found in a wide number of other neoplasms that include for example melanoma and a large number of breast carcinomas.

The identification of different subtypes of malignant peripheral nerve sheath tumors will force us to analyze more MPNSTs on gene microarrays than we have done so far. To this extent we have contacted Dr. Andre Oliveira and Dr. Bernd Scheithauer at the Mayo Clinic in Rochester who have access to large numbers of these tumors. They have enthusiastically agreed to collaborate with us on this project and currently we are near the end of a process to obtain IRB approval to accept these specimens. We subsequently will apply for approval from the Department of Defense through Dr. Inez Beitin's office.

In the past year we have not performed any comparative genomic hybridization analyses because we wanted to perform the gene expression profiling first. However all specimens that have been analyzed for gene expression profiling also have their DNA isolated and in the next year we expect to analyze these on cDNA microarrays to look for gene copy number loss and gain.

In a remarkable collaboration among the three collaborating institutions on this grant (Stanford University Medical Center, University of British Columbia, University of Washington), we have been able to generate what we believe is the largest nerve sheath tumor tissue microarray that is currently available. From this array three copies were made and one block each is now located at each institution. We have performed a number of in situ hybridizations on this so far without success in finding a "golden bullet" to identify all MPNSTs but we have great hopes that additional analyses will find one or more genes that will assist in the positive identification of MPNSTs. Our collaborator Dr. Torsten Nielsen at the University of British Columbia has been successful in finding an antibody against all forms of TLE (based on our gene array data and that from Dr. Marc Ladanyi at the Memorial Sloan-Kettering Cancer Center) that positively identifies the major differential diagnostic tumor for MPNST namely synovial sarcoma. We are currently using in situ hybridization probes to determine if the antiserum used by Dr. Nielsen is a commercially available one that reacts with all isoforms of the TLE gene. We are currently generating in situ hybridization probes to see which variant(s) of the TLE gene family is the best marker for synovial sarcoma.

REFERENCES

Cichowski K, Jacks T. NF1 tumor suppressor gene function: narrowing the GAP. Cell. 2001; 104:593-604.

Eisen MB, Spellman PT, Brown PO, Botstein D. Cluster analysis and display of genome-wide expression patterns. Proc Natl Acad Sci U S A. 1998; 95:14863-8.

Gilks CB, Vanderhyden BC, Zhu S, van de Rijn M, Longacre TA. Distinction between serous tumors of low malignant potential and serous carcinomas based on global mRNA expression profiling. Gynecol Oncol. 2005; 96:684-94.

Massague J. How cells read TGF-beta signals. Nat Rev Mol Cell Biol. 2000; 1:169-78.

Nielsen TO, Hsu FD, Jensen K, Cheang M, Karaca G, Hu Z, Hernandez-Boussard T, Livasy C, Cowan D, Dressler L, Akslen LA, Ragaz J, Gown AM, Gilks CB, van de Rijn M, Perou CM. Immunohistochemical and clinical characterization of the basal-like subtype of invasive breast carcinoma. Clin Cancer Res. 2004;10:5367-74.

Riccardi VM. Von Recklinghausen neurofibromatosis. N Engl J Med. 1981; 305:1617-27.

Subramanian S, West RB, Corless CL, Ou W, Rubin BP, Chu KM, Leung SY, Yuen ST, Zhu S, Hernandez-Boussard T, Montgomery K, Nielsen TO, Patel RM, Goldblum JR, Heinrich MC, Fletcher JA, van de Rijn M. Gastrointestinal stromal tumors (GISTs) with KIT and PDGFRA mutations have distinct gene expression profiles. Oncogene. 2004; 23:7780-90.

Subramanian S, West RB, Marinelli RJ, Nielsen TO, Rubin BP, Goldblum JR, Patel RM, Zhu S, Montgomerry K, Ng TL, Corless CL, Heinrich MC, van de Rijn M. The gene expression profile of extraskeletal myxoid chondrosarcoma. J Pathol 2005; (in press).

Tusher VG, Tibshirani R, Chu G. Significance analysis of microarrays applied to the ionizing radiation response. Proc Natl Acad Sci U S A. 2001; 98:5116-21.

van de Rijn M, Perou CM, Tibshirani R, Haas P, Kallioniemi O, Kononen J, Torhorst J, Sauter G, Zuber M, Kochli OR, Mross F, Dieterich H, Seitz R, Ross D, Botstein D, Brown P. Expression of cytokeratins 17 and 5 identifies a group of breast carcinomas with poor clinical outcome. Am J Pathol. 2002;161:1991-6.

West RB, Harvell J, Linn SC, Liu CL, Prapong W, Hernandez-Boussard T, Montgomery K, Nielsen TO, Rubin BP, Patel R, Goldblum JR, Brown PO, van de

Rijn M. Apo D in soft tissue tumors: a novel marker for dermatofibrosarcoma protuberans. Am J Surg Pathol. 2004; 28:1063-9.

West RB, Corless CL, Chen X, Rubin BP, Subramanian S, Montgomery K, Zhu S, Ball CA, Nielsen TO, Patel R, Goldblum JR, Brown PO, Heinrich MC, van de Rijn M. The novel marker, DOG1, is expressed ubiquitously in gastrointestinal stromal tumors irrespective of KIT or PDGFRA mutation status.
Am J Pathol. 2004;165:107-13.

West RB, Nuyten DS, Subramanian S, Nielsen TO, Corless CL, Rubin BP, Montgomery K, Zhu S, Patel R, Hernandez-Boussard T, Goldblum JR, Brown PO, Vijver MV, Rijn MV. Determination of stromal signatures in breast carcinoma. PLoS Biol. 2005; 3(6):e187

APPENDICES

None